

Design and Simplification of Quantize-Forward Relaying in Massive MIMO HetNets

Ahmad Abu Al Haija*, Min Dong[‡], Ben Liang*, Gary Boudreau[†], S. Hossein Seyedmehdi[†]

* University of Toronto, Toronto, ON, Canada, [†]Ericsson Canada, Ottawa, ON, Canada

[‡] University of Ontario Institute of Technology, Oshawa, ON, Canada

Abstract—To investigate how massive multiple-input multiple-output (MIMO) impacts the data transmission of a dense heterogeneous network (HetNet), we study its uplink transmission that consists of two users communicating with a macro-cell base station (MCBS) through a small-cell BS (SCBS) with zero-forcing (ZF) detection at each BS. We first analyze the scheme with quantize-forward (QF) relaying at the SCBS and joint decoding (JD) at the MCBS for both users' messages. To maximize the rate region, we derive the optimal quantization at the SCBS for both users' data streams and show how they depend on the large-scale fading. We further propose a new scheme that simplifies the QF-JD scheme through Wyner-Ziv (WZ) binning and time division (TD) transmission at the SCBS to allow not only sequential but also separate decoding of each user's message at the MCBS. For this QF-WZTD scheme, the optimal quantization parameters are identical to that of the QF-JD scheme while the phase durations and power allocation are conveniently optimized as functions of the quantization parameters. Despite its simplicity, the QF-WZTD scheme achieves the same rate region of the QF-JD scheme, making it an attractive option for the fifth-generation HetNets.

I. INTRODUCTION

The development of the fifth-generation (5G) cellular networks aims to drastically improve the spectral efficiency and data rate of current networks to serve an escalating number of connected devices. Hence, some key enabling technologies have been proposed, such as Ultra Dense Networks (UDNs), HetNets, massive MIMO, and full-duplex transmission [1].

In UDNs, the number of user equipments (UEs) is small as compared with the number of SCBSs and MCBSs [2]. Hence, we investigate the uplink transmission in a HetNet as shown in Fig. 1, where two UEs communicate with a MCBS through a SCBS. This uplink channel theoretically resembles the multiple-access relay channel (MARC) [3]. With a single antenna at each node, the rate regions for MARC have been derived for decode-forward (DF) relaying [3], [4] and QF relaying [5]–[7] schemes. In an UDN, the SCBS location is random and can be close the MCBS where QF relaying can outperform DF relaying [8]. Hence, in this paper, we investigate QF relaying in a massive MIMO HetNet.

For multi-antenna QF relaying, the quantization resolution at the relay node is the key design problem. This leads to the optimization of the covariance matrix of the quantization noise vector, which is in general non-convex and challenging. Hence, approximate solutions were obtained via iterative numerical methods for one way [9] and two way [10] half-duplex relay channels and cloud radio access network [11]. With massive

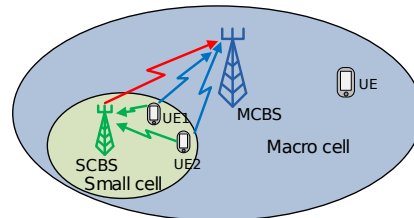


Fig. 1. Uplink transmission in a dense HetNet.

MIMO, the quantization problem can be simplified with possible closed-form solutions, avoiding high computational cost and processing delay of the numerical methods.

The design simplification with massive MIMO [12] stems from its ability to 1) neglect the small scale fading through channel hardening [13], 2) orthogonalize different user transmissions through beamforming [14], and 3) approach the optimal performance with simple linear receivers, e.g. zero forcing (ZF) receiver [14]. Consequently, the optimal design of quantization noise covariance may only depend on the large-scale fading of each channel with a complexity that scales with the number of UEs instead of antennas [12, Myth 9]. Since large-scale antenna arrays can be made rather compact, they can be implemented at both MCBS and SCBS [12] [15]. Hence, it is of interest to investigate how massive MIMO simplifies the QF relaying design in a HetNet.

This paper has the following contributions:

- We consider the uplink transmission of two UEs in a massive MIMO HetNet with ZF detection and analyze the rate region of a QF-JD scheme with QF relaying at the SCBS and JD at the MCBS for both UEs' messages. To maximize the rate region, we derive the optimal quantization parameters at the SCBS for UEs' data streams in closed-form, where the number of parameters is equal to the number of UEs instead of antennas, and we show how their values depend on the large-scale fading [12].
- We propose a new QF-WZTD scheme that simplifies QF-JD by deploying not only Wyner-Ziv (WZ) binning at the SCBS [8] but also time division (TD) transmission for each bin index of a UE's quantized data stream. These two techniques allow the the MCBS to deploy separate and sequential decoding for each bin index, quantization index, and UE message.
- We prove that the proposed QF-WZTD scheme has the same rate region and the same optimal quantization parameters as those of the QF-JD scheme, while the optimal TD phase durations and power allocation are conveniently obtained as direct functions of the quantization parameters.

II. CHANNEL MODEL

We consider the uplink transmission in a HetNet that consists of a MCBS, a SCBS, and two UEs (UE₁ and UE₂). We ignore the other SCBSs and their UEs as applying massive MIMO technology at both MCBS and SCBS can reduce the uplink interference from the other nodes to negligible levels [14]. Each UE has a single antenna while the SCBS (resp.~MCBS) has N (resp.~ M) antennas where we assume $M \gg N \gg 1$. The two UEs communicate with the MCBS through the SCBS, as shown in Fig. 1. This uplink channel resembles the MARC shown in Fig. 2 where the SCBS resembles the relay (\mathcal{R}) and the MCBS resembles the destination (\mathcal{D}).

For MARC in Fig. 2, we assume a block fading channel model where the links remain constant in each transmission block and change independently between blocks. Hence, over multiple transmission blocks, e.g., B blocks where $B \gg 1$), let $\mathbf{h}_{r,i,j}$ denote the $N \times 1$ channel coefficient vector from UE _{i} to \mathcal{R} in block j for $i \in \{1, 2\}$ and $j \in \{1, \dots, B\}$. Then, the n^{th} element of this vector $h_{r,i,j}^{(n)}$ denotes the channel coefficient from UE _{i} to the n^{th} antenna of \mathcal{R} in block j . This channel coefficient is a complex Gaussian random variable with zero mean and variance $\sigma_{h,r}^2$. We model the variance using the pathloss model as $\sigma_{h,r}^2 = d_{r,i}^\alpha$, where $d_{r,i}$ is the distance between UE _{i} and \mathcal{R} , and α is the pathloss exponent. A Similar definition holds for each element of the $M \times 1$ channel coefficient vector $\mathbf{h}_{d,i,j}$ from UE _{i} to \mathcal{D} and the $M \times N$ channel matrix \mathbf{H}_{dr} from \mathcal{R} to \mathcal{D} . We assume all channel coefficients are independent to each other.

Therefore, at any transmission block $j \in \{1, \dots, B\}$ with channel coefficients $\mathbf{h}_{r,i,j}$, $\mathbf{h}_{d,i,j}$ and $\mathbf{H}_{dr,j}$, the system equations of MARC in Fig. 2 are given as follows:

$$\begin{aligned} \mathbf{y}_{r,j} &= \mathbf{h}_{r1,j}x_{1,j} + \mathbf{h}_{r2,j}x_{2,j} + \mathbf{z}_{r,j}, \\ \mathbf{y}_{d,j} &= \mathbf{h}_{d1,j}x_{1,j} + \mathbf{h}_{d2,j}x_{2,j} + \mathbf{H}_{dr,j}\mathbf{x}_{r,j} + \mathbf{z}_{d,j}, \end{aligned} \quad (1)$$

where $\mathbf{y}_{r,j}$ (resp.~ $\mathbf{y}_{d,j}$) is the $N \times 1$ (resp.~ $M \times 1$) received signal vector at \mathcal{R} (resp.~ \mathcal{D}); $x_{i,j}$ is the transmit signal by UE _{i} for $i \in \{1, 2\}$ while $\mathbf{x}_{r,j}$ is the $N \times 1$ transmit signal vector from \mathcal{R} ; $\mathbf{z}_{r,j} \in C^{N \times 1}$ and $\mathbf{z}_{d,j} \in C^{M \times 1}$ are independent complex AWGN vectors with zero mean and covariance \mathbf{I}_N and \mathbf{I}_M , respectively.

We assume that the channel state information is known at the respective receivers (\mathcal{R}, \mathcal{D}), i.e. \mathcal{R} knows $\mathbf{h}_{r,i}$ while \mathcal{D} knows $\mathbf{h}_{d,i}$ and \mathbf{H}_{dr} . Moreover, \mathcal{R} knows (via feedback from \mathcal{D} [16]) its distance to \mathcal{D} and the distance of each UE to \mathcal{D} such that it can optimize its transmission for maximum spectral efficiency (see Sections IV and V).

Although full-duplex relaying at the SCBS suffers from self-interference, it can be substantially alleviated by analog and digital cancellation techniques, and the remaining part appears as an additional additive noise [17]. Hence, we ignore the self-interference at the SCBS and focus on its transmission design.

For a system with massive MIMO, it is known [14] that inter-user interference diminishes and high data rate is achievable by low complexity linear detectors such as ZF, maximum ratio combining (MRC) and minimum-mean-square-error (MMSE). In this paper, we choose ZF detector for simplicity; but similar analysis is applicable to other detectors. \mathcal{R}

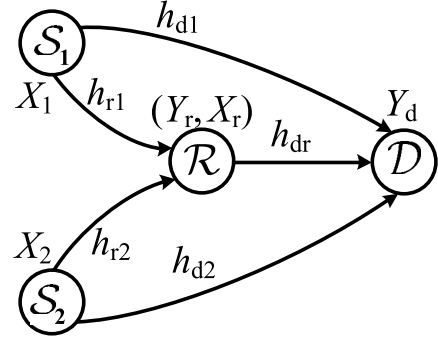


Fig. 2. The channel model of full-duplex MARC.

(resp. \mathcal{D}) deploys ZF detection to separate data streams from different users by multiplying its received signal vector $\mathbf{y}_{r,j}$ (resp. $\mathbf{y}_{d,j}$) in (1) with $\mathbf{A}_{r,j}$ (resp. $\mathbf{A}_{d,j}$), for $j \in \{1, \dots, B\}$ where

$$\begin{aligned} \mathbf{A}_{r,j} &\triangleq (\mathbf{G}_{r,j}^H \mathbf{G}_{r,j})^{-1} \mathbf{G}_{r,j}^H, \quad \mathbf{A}_{d,j} \triangleq (\mathbf{G}_{d,j}^H \mathbf{G}_{d,j})^{-1} \mathbf{G}_{d,j}^H, \\ \mathbf{G}_{r,j} &\triangleq [\mathbf{h}_{r1,j} \quad \mathbf{h}_{r2,j}], \quad \mathbf{G}_{d,j} \triangleq [\mathbf{h}_{d1,j} \quad \mathbf{h}_{d2,j} \quad \mathbf{H}_{dr,j}]. \end{aligned} \quad (2)$$

Then, let $\mathbf{A}_{r,j} = [\mathbf{a}_{r1,j}, \mathbf{a}_{r2,j}]^H$ and $\mathbf{A}_{d,j} = [\mathbf{a}_{d1,j}, \mathbf{a}_{d2,j}, \mathbf{A}_{dr,j}]^H$, where $\mathbf{a}_{r,i,j}$ is an $N \times 1$ vector, $\mathbf{a}_{d,i,j}$ is an $M \times 1$ vector, for $i \in \{1, 2\}$, and $\mathbf{A}_{dr,j}$ is an $M \times N$ matrix. After applying ZF detection in (2) into (1), we obtain the 2×1 received vector $\tilde{\mathbf{y}}_{r,j}$ at \mathcal{R} and $(2+N) \times 1$ received vector $\tilde{\mathbf{y}}_{d,j}$ at \mathcal{D} as follows

$$\begin{aligned} \tilde{\mathbf{y}}_{r,j} &= [\tilde{y}_{r1,j} \quad \tilde{y}_{r2,j}]^T, \quad \tilde{\mathbf{y}}_{d,j} = [\tilde{y}_{d1,j} \quad \tilde{y}_{d2,j} \quad \tilde{\mathbf{y}}_{dr,j}]^T, \\ \tilde{y}_{ri,j} &= x_{i,j} + \mathbf{a}_{ri,j}^H \mathbf{z}_{r,j}, \quad \tilde{y}_{di,j} = x_{i,j} + \mathbf{a}_{di,j}^H \mathbf{z}_{d,j}, \quad i \in \{1, 2\} \\ \tilde{\mathbf{y}}_{dr,j} &= \mathbf{x}_{r,j} + \mathbf{A}_{dr,j}^H \mathbf{z}_{d,j}. \end{aligned} \quad (3)$$

where $\tilde{y}_{ri,j}$ (resp.~ $\tilde{y}_{di,j}$) is the data stream received at \mathcal{R} (resp.~ \mathcal{D}) from UE _{i} , and $\tilde{\mathbf{y}}_{dr,j}$ is the $N \times 1$ data stream vector received at \mathcal{D} from \mathcal{R} .

III. QF-JD SCHEME FOR MASSIVE MIMO HETNET

Since massive MIMO asymptotically orthogonalizes the transmissions from different users [14], the SCBS can separately quantize the data stream from each UE as in [8]. The MCBS then utilizes the received signals from both UEs and the SCBS to improve the spectral efficiency.

In the QF-JD scheme, the transmission is carried over B independent blocks where each UE aims to send $B-1$ messages through B transmission blocks. In each block, each UE transmits new information; the SCBS quantizes the received data stream from each UE in (3), and sends the quantization indices to the MCBS in the next block; then the MCBS performs sliding window decoding over two consecutive blocks.

A. Transmission Scheme

In transmission block $j \in \{1, 2, \dots, B\}$, UE₁ sends its new message $w_{1,j}$ by transmitting its codeword U_1 . Similarly, UE₂ sends $w_{2,j}$ by transmitting U_2 . At the end of block j , the SCBS first deploys ZF detection for its received signal $\mathbf{y}_{r,j}$. Then, it quantizes the detector's output signals $\tilde{y}_{r1,j}$ and $\tilde{y}_{r2,j}$ and determines the quantization indices (l_j, k_j) . Finally, the SCBS generates a common codeword U_r for both indices (l_j, k_j) and transmits it in block $j+1$ to the MCBS. Similarly, the SCBS transmits $U_r(l_{j-1}, k_{j-1})$ in block j .

1) *Transmitted Signals*: During transmission block j , UE₁, UE₂, and the SCBS respectively transmit $x_1(w_{1,j})$, $x_2(w_{2,j})$ and $\mathbf{x}_r(l_{j-1}, k_{j-1})$. They construct their signals as follows.

$$\begin{aligned} x_{i,j} &= \sqrt{P_i} U_i(w_{i,j}), \quad i \in \{1, 2\}, \\ \mathbf{x}_{r,j} &= \sqrt{P_r/N} \mathbf{U}_r(l_{j-1}, k_{j-1}), \quad \hat{y}_{ri,j} = \tilde{y}_{ri,j} + \hat{z}_{ri,j}, \end{aligned} \quad (4)$$

where $\hat{y}_{ri,j}$, for $i \in \{1, 2\}$ is the quantized version of $\tilde{y}_{ri,j}$ in (3) and $\hat{z}_{ri,j}$ is the quantization noise which is zero mean Gaussian with variance Q_i . U_1 and U_2 are i.i.d Gaussian signals with zero mean and unit variance and they respectively convey the codewords of UEs' messages $w_{1,j}$ and $w_{2,j}$. \mathbf{U}_r and is an $N \times 1$ Gaussian signal vector with zero mean and covariance \mathbf{I}_N and it conveys the codeword of the quantization index pair (l_{j-1}, k_{j-1}) . The transmit powers at UE₁, UE₂, and the SCBS are P_1 , P_2 and P_r , respectively.

2) *Decoding*: Based on maximum likelihood (ML) [18] or joint typicality (JT) [8] decoding methods as in Appendix A, The MCBS jointly decodes both UEs' messages as follows.

The MCBS performs sliding window decoding over two consecutive blocks (j and $j+1$) to decode both UEs information and the quantization indices from the SCBS. Specifically, at the end of block $j+1$, after performing ZF detection in (3), the MCBS simultaneously utilizes the received signals from both UEs in block j ($\tilde{y}_{d1,j}$ and $\tilde{y}_{d2,j}$) and from the SCBS in block $j+1$ ($\tilde{\mathbf{y}}_{dr,j+1}$) to jointly decode both UEs information ($w_{1,j}, w_{2,j}$) for some quantization indices (l_j, k_j) .

B. Achievable Rate Region

The rate constraints that insure reliable decoding at the MCBS determine the achievable rate region as follows.

Theorem 1. *For the considered massive MIMO HetNet, the QF-JD scheme achieves a rate region that consists of all rate pairs (R_1, R_2) satisfying*

$$R_1 \leq \min\{I_1, I_2\}, \quad R_2 \leq \min\{I_3, I_4\}, \quad R_1 + R_2 \leq I_5, \quad (5)$$

where

$$\begin{aligned} I_1 &= \mathcal{C} \left(P_1(M-N)d_{d1}^{-\alpha} + P_1 / \left((d_{r1}^{\alpha}/N) + Q_1 \right) \right), \\ I_2 &= \mathcal{C} \left(P_1(M-N)d_{d1}^{-\alpha} \right) + \zeta, \quad I_4 = \mathcal{C} \left(P_2(M-N)d_{d2}^{-\alpha} \right) + \zeta, \\ I_3 &= \mathcal{C} \left(P_2(M-N)d_{d2}^{-\alpha} + P_2 / \left((d_{r2}^{\alpha}/N) + Q_2 \right) \right), \\ I_5 &= \mathcal{C} \left(P_1(M-N)d_{d1}^{-\alpha} \right) + \mathcal{C} \left(P_2(M-N)d_{d2}^{-\alpha} \right) + \zeta, \\ \zeta &\triangleq N\mathcal{C} \left(\frac{P_r(M-N)}{Nd_{dr}^{\alpha}} \right) - \mathcal{C} \left(\frac{d_{r1}^{\alpha}}{NQ_1} \right) - \mathcal{C} \left(\frac{d_{r2}^{\alpha}}{NQ_2} \right) \end{aligned} \quad (6)$$

and $\mathcal{C}(x) \triangleq \log(1+x)$.

Proof: The constraints ensure reliable decoding for both UEs' messages at the MCBS, see Appendix A for details. ■

Theorem 1 shows that massive MIMO simplifies the quantization process at the SCBS compared to a regular MIMO system. Unlike a regular MIMO system which requires optimizing the covariance matrix of the quantization noise vector [9], [10] to obtain the rate region boundaries, the massive MIMO system only requires two quantization elements to be optimized. This simplification coincides with [12, Myth 9] that in the massive MIMO system, the complexity of resource allocation scales with the number of UEs instead of antennas.

IV. OPTIMAL QUANTIZATION (Q_1^*, Q_2^*)

For practical implementation, it is important to specify the optimal quantization at the SCBS for each UE data stream. As the quantization levels increase, the quantizer becomes finer with smaller noises (Q_1, Q_2) at its outputs ($\hat{y}_{r1,j}, \hat{y}_{r2,j}$) in (4). Therefore, we derive here the optimal parameters (Q_1^*, Q_2^*) that maximize the rate region in (5).

In Theorem 1, any boundary point of the rate region can be represented by the weighted sum rate $\mu_1 R_1 + \mu_2 R_2$, where $\mu_1 \in [0, 1]$ is some priority weighting factor of UE₁ rate, and $\mu_2 = 1 - \mu_1$. Thus, the rate region boundary is achieved by maximizing the weighted sum rate for some given μ_1 over Q_1 and Q_2 . Hence, the optimization problem is formulated as

$$\max_{Q_1, Q_2} \mu_1 R_1 + \mu_2 R_2, \quad \text{s.t. } R_1 \leq \min\{I_1, I_2\}, \quad (7)$$

$$R_2 \leq \min\{I_3, I_4\}, \quad R_1 + R_2 \leq I_5, \quad Q_1 \geq 0, \quad Q_2 \geq 0,$$

where I_1, I_2, \dots, I_5 are given in (6) with full transmission powers as in (4). The solution of (7) is given as follows.

Theorem 2. *For $k \in \{1, 2\}$, the optimal Q_k^* that solves problem (7) is given as*

$$Q_k^* = \frac{(d_{rk}^{\alpha}/N)(1 + P_k(M-N)d_{dk}^{-\alpha}) + P_k}{(1 + P_k(M-N)d_{dk}^{-\alpha})(\lambda_k - 1)}, \quad (8)$$

where $\lambda_1 = (2A)^{-1}(B + \sqrt{B^2 - 4AC})$, $\lambda_2 = \lambda_s/\lambda_1$,

$$\text{with } A = \mu_2 P_2 (d_{r1}^{\alpha}/N) (1 + P_1(M-N)d_{d1}^{-\alpha}),$$

$$C = -\mu_1 P_1 (d_{r2}^{\alpha}/N) (1 + P_2(M-N)d_{d2}^{-\alpha}) \lambda_s,$$

$$B = (\mu_1 - \mu_2) P_1 P_2, \quad \text{and } \lambda_s = (1 + P_r(M-N)/(Nd_{dr}^{\alpha}))^N,$$

But if $\lambda_1 < 1$ (resp. $\lambda_1 > \lambda_s$), set $\lambda_1 = 1$ (resp. $\lambda_1 = \lambda_s$).

Proof: 1) Considering (5), for $\mu_1 \in (0.5, 1]$, the weighted sum rate $R_{ws} = \mu_1 R_1 + \mu_2 R_2$ can be expressed as follows:

$$R_{ws} = (\mu_1 - \mu_2) R_1 + \mu_2 (R_1 + R_2), \quad (9)$$

$$\stackrel{a}{\leq} (\mu_1 - \mu_2) \min\{I_1, I_2\} + \mu_2 \min\{I_1 + I_3, I_5\},$$

$$\stackrel{b}{=} \begin{cases} \mu_1 I_1 + \mu_2 I_3 & \text{if } I_1 \leq I_2, \text{ \& } I_1 + I_3 \leq I_5, \\ (\mu_1 - \mu_2) I_2 + \mu_2 I_5 & \text{if } I_1 > I_2, \text{ \& } I_1 + I_3 > I_5, \\ (\mu_1 - \mu_2) I_2 + \mu_2 (I_1 + I_3) & \text{if } I_1 > I_2, \text{ \& } I_1 + I_3 \leq I_5, \\ (\mu_1 - \mu_2) I_1 + \mu_2 I_5 & \text{if } I_1 \leq I_2, \text{ \& } I_1 + I_3 > I_5 \end{cases},$$

where (a) follows from the rate constraints in (7) while (b) follows from all four possible cases of (a) at any Q_1 and Q_2 and by noticing that $I_1 + I_4 > I_5$ and $I_2 + I_3 > I_5$.

2) We maximize each case in (9.b) subject to its constraints and then choose the case that maximizes R_{ws} . For,

- Case 1: the constraint $I_1 \leq I_2$ is redundant when $I_1 + I_3 \leq I_5$. Hence, the optimization problem becomes:

$$\max_{Q_1, Q_2} \mu_1 I_1 + \mu_2 I_3, \quad \text{s.t. } I_1 + I_3 = I_5, \quad Q_1 \geq 0, \quad Q_2 \geq 0. \quad (10)$$

Since I_1 (I_3) is a decreasing function with Q_1 (Q_2) while I_5 is increasing with both Q_1 and Q_2 , R_{ws} is maximized when $I_1 + I_3 \leq I_5$ holds with equality.

- Case 2 is equivalent to individual rate maximization of UE₁ (denote as R_1^{\max}), since $I_1 + I_3 > I_5$ is redundant when $I_1 > I_2$. Moreover, R_{ws} is independent of Q_2 since $(\mu_1 - \mu_2) I_2 + \mu_2 I_5 = \mu_1 I_2 + \mu_2 \mathcal{C}((P_2(M-N))/(d_{d2}^{\alpha}))$.

- Case 3 is also equivalent to R_1^{\max} , since besides the constraint $I_1 + I_3 > I_5$ and $I_1 \leq I_2$, it is clear from (5) that $I_5 - I_3 \leq I_2$. Hence, these three inequalities only hold when they are equal $I_5 - I_3 = I_1 = I_2$, which is possible only when $Q_2 \rightarrow \infty$, i.e. R_1^{\max} .
- Case 4, $R_{ws} = (\mu_1 - \mu_2)I_1 + \mu_2 I_5$ is maximized with maximum possible Q_2 (obtained when $I_1 + I_3 = I_5$).

Therefore, considering the four cases, the optimization problem in (7) is equivalent to (10).

- 3) Considering I_5 in (10), let $NC(P_r(M - N)/(Nd_{dr}^\alpha)) = \log(\lambda_s) = \log(\lambda_1) + \log(\lambda_2)$, where λ_s is given in (8) while $\lambda_1 \lambda_2 = \lambda_s$. Then, from the constraint $I_1 + I_3 = I_5$, we obtain Q_1 and Q_2 as in (8).
- 4) By substituting Q_1 and Q_2 in (8) into (10), the optimization problem in (10) becomes as follows:

$$\begin{aligned} & \max_{\lambda_1, \lambda_2} \mu_1 I_1 + \mu_2 I_3, \text{ s.t. } \lambda_1 \lambda_2 = \lambda_s, \lambda_1 \geq 1, \lambda_2 \geq 1 \\ & \text{with } I_1 = \mathcal{C}(P_1(M - N)/d_{d1}^\alpha) + \mathcal{C}(P_1(M - N)/d_{r1}^\alpha) \\ & \quad - \mathcal{C}(P_1(M - N)d_{d1}^{-\alpha} + P_1 N \lambda_1^{-1} d_{r1}^{-\alpha}), \end{aligned} \quad (11)$$

and I_3 has similar expression to I_1 except for switching each subscript from 1 to 2 and the condition $\lambda_i \geq 1$ ensures that $Q_i \geq 0$. Since I_1 depends on λ_1 only in the negative term, (11) can be reexpressed as follows:

$$\begin{aligned} & \min_{\lambda_1, \lambda_2} \sum_{i=1}^2 \mu_i \log(1 + P_i(M - N)d_{di}^{-\alpha} + P_i N \lambda_i^{-1} d_{ri}^{-\alpha}) \\ & \text{s.t. } \lambda_1 \lambda_2 = \lambda_s, \lambda_1 \geq 1, \lambda_2 \geq 1. \end{aligned} \quad (12)$$

- 5) By substituting $\lambda_2 = \lambda_s/\lambda_1$ into (12) and then deriving (12) with respect to λ_1 , we obtain λ_1^* as a solution of

$$f_1(\lambda_1) = 0, \text{ where } f_1(\lambda_1) = A\lambda_1^2 - B\lambda_1 + C, \quad (13)$$

while A, B and C are given in (8). If λ_1 from (13) is < 1 (resp. $> \lambda_s$), the function in (12) is increasing (resp. decreasing) over $\lambda_1 \in [1, \lambda_s]$, then $\lambda_1^* = 1$ (resp. λ_s). ■

Remark 1. Theorem 2 has several implications:

- It includes the following special cases:
 - Maximum individual rate R_i^{\max} (for $i \in \{1, 2\}$) is obtained by setting $\mu_i = 1$. With $\mu_2 = 0$, the function in (12) is decreasing with λ_1 . Hence, $(\lambda_1^*, \lambda_2^*) = (\lambda_s, 1)$. Consequently, Q_1^* is as in (8) while $Q_2^* \rightarrow \infty$ (i.e. not relaying the signal from UE₂). Therefore, R_1^{\max} is achieved when the SCBS optimally QF the received signal from UE₁ and ignores that from UE₂, which is received at the MCBS through the direct link only.
 - Maximum throughput (sum rate) when $\mu_1 = \mu_2 = 0.5$.
- The optimal quantization depends on the large-scale fading (distances and path loss exponents). The MCBS can feedback this information to the SCBS which is much simpler than sending the instantaneous CSI for all channel vectors.

V. QF-WZTD SCHEME

The QF-JD scheme in Section III deploys 1) a common codeword \mathbf{U}_r for both quantization indices at the SCBS to be transmitted to the MCBS, and 2) JD of both UEs' messages at the MCBS. This results in exponential computational

complexity with the number of UEs at both SCBS and MCBS [8]. Specifically, let K_i be the set of quantization indices for UE _{i} data stream where $i \in \{1, 2\}$, then $K_1 \times K_2$ will be the codebook size for all pairs of quantization indices, i.e. a common codeword for each pair. Similar complexity holds with JD at the MCBS.

Practical systems, however, often prefer a low-complexity design which involves 1) separate codeword transmission (i.e. $K_1 + K_2$ codewords), and 2) separate and sequential decoding. Simpler techniques are feasible when the SCBS, besides the quantization, deploys TD transmission along with WZ binning for the quantization indices. While TD allows separate codeword transmission and separate decoding, WZ binning allows sequential decoding [8] as shown next.

A. QF-WZTD Transmission Scheme

Each UE transmission is identical to that in Section III, but the SCBS transmission and the MCBS decoding are different.

1) At the SCBS: WZ binning and TD transmission:

- First, the SCBS deploys WZ binning where it partitions the quantization indices for each UE data stream into equal-size bins [8]. That is, after performing ZF detection and determining the quantization indices (l_j, k_j) as in Section III, the SCBS finds the two binning indices $b_{1,j}$ and $b_{2,j}$ that include l_j and k_j , respectively.
- Second, the SCBS deploys TD transmission where it generates separate codewords U_{r1} and U_{r2} for binning indices $b_{1,j}$ and $b_{2,j}$, respectively, and transmits them in block $j + 1$ in two separate phases of fractions of block duration β_1 and β_2 , respectively. Therefore, in transmission block j , the SCBS generates its signals for forwarding as follows:

$$\text{Phase } i: \mathbf{x}_{ri,j} = \sqrt{\rho_{ri}/(\beta_1 N)} \mathbf{U}_{ri}(b_{i,j-1}), \quad i \in \{1, 2\} \quad (14)$$

where $\beta_1 + \beta_2 = 1$ and $\rho_{r1} + \rho_{r2} = P_r$. Note that the SCBS also deploys power control as it transmits with powers (ρ_{r1}/β_1) in phase 1 and (ρ_{r2}/β_2) in phase 2, respectively.

2) *Decoding at the MCBS:* The MCBS performs sliding window decoding to separately and sequentially decode each bin index, quantization index and then each UE message. Specifically, after ZF detection in (3), the received signals over two phases in block $j + 1$ from the SCBS are given as follows:

$$\text{Phase } i: \tilde{\mathbf{y}}_{dri,j+1} = \mathbf{x}_{ri,j+1} + \mathbf{A}_{dr,j+1}^H \mathbf{z}_{di,j+1}, \quad i \in \{1, 2\} \quad (15)$$

As both UEs have similar decoding, for UE₁, the MCBS sequentially decodes: 1) the bin index $\hat{b}_{1,j}$ using $\tilde{\mathbf{y}}_{dr1,j+1}$, 2) the quantization index \hat{l}_j using $\tilde{\mathbf{y}}_{d1,j}$ given that $\hat{l}_j \in b_{1,j}$, and then 3) UE₁ message $\hat{w}_{1,j}$ using $\tilde{\mathbf{y}}_{d1,j}$ and $\hat{\mathbf{y}}_{r1,j}(\hat{l}_j)$.

B. Achievable Rate Region

The rate constraints that ensure reliable decoding at the MCBS determine the spectral efficiency region as follows.

Theorem 3. *For massive MIMO HetNets, the QF-WZTD scheme achieves a rate region that consists of all rate pairs (R_1, R_2) satisfying*

$$R_1 \leq I_1, \quad R_2 \leq I_3, \quad (16)$$

$$\begin{aligned} & \text{s.t. } L_i \leq \beta_i NC(\rho_{ri}(M - N)/(\beta_i N d_{dr}^\alpha)), \quad i \in \{1, 2\} \\ & \beta_1 + \beta_2 = 1, \quad \rho_{r1} + \rho_{r2} = P_r, \end{aligned} \quad (17)$$

$$\text{where } L_i = \mathcal{C} \left(\frac{1}{Q_i} \left[\frac{d_{ri}^\alpha}{N} + \frac{P_i}{1 + (P_i(M-N)/d_{di}^\alpha)} \right] \right),$$

while (I_1, I_3) are given in (6).

Proof: Similar to Appendix A but with the signaling and decoding rule in Sections V-A1 and V-A2, respectively. We omit the detailed proof because of space limitation. ■

1) *Comparison with the QF-JD scheme:* Generally, simple sequential and separate decoding results in a smaller rate region than that under the joint decoding [8]. However, for the considered HetNet, we obtain the following theorem:

Theorem 4. *In massive MIMO HetNets, the simple QF-WZTD scheme achieves the same rate region of the QF-JD scheme.*

Proof: Both schemes achieve the same weighted sum rate since the two constraints in (16) lead to the same Q_1^* and Q_2^* in (8) except replacing λ_i by λ_{si} for $i \in \{1, 2\}$ where

$$\lambda_{si} = (1 + \rho_{ri}(M-N)/(\beta_i N d_{dr}^\alpha))^{\beta_i N}. \quad (18)$$

Hence, the two schemes achieve the same maximum weighted sum rate when $\lambda_{si} = \lambda_i^*$ in (8), which is possible by setting

$$\beta_i^* = (\rho_{ri}^*/P_r), \quad \rho_{ri}^* = (\log(\lambda_i^*)/\log(\lambda_s))P_r, \quad i \in \{1, 2\}. \quad (19)$$

where (19) satisfies the conditions in (17). ■

Remark 2. Compared with the QF-JD scheme, the QF-WZTD scheme require no more optimization as its extra parameters of the phase durations and power allocation are simply optimized as functions of the optimal quantization for the QF-JD scheme.

2) *Comparison with DF relaying [3]:* The SCBS decodes both UEs' messages and forwards them to the MCBS that jointly decodes both messages using sliding window decoding. The achievable rate region then becomes as follows:

Proposition 1. *For massive MIMO HetNets, the DF-JD scheme achieves a rate region that consists of all rate pairs (R_1, R_2) satisfying*

$$R_1 \leq \min\{T_1, T_2\}, \quad R_2 \leq \min\{T_3, T_4\}, \quad R_1 + R_2 \leq T_5, \\ \text{where } T_1 = \mathcal{C}(P_1 N / (d_{r1}^\alpha)), \quad T_3 = \mathcal{C}(P_2 N / (d_{r2}^\alpha)), \quad (20)$$

while T_2, T_4 and T_5 are respectively similar to I_2, I_4 and I_5 in (6) except modifying ζ by keeping the first term only.

Proof: T_1 and T_3 (resp. T_2, T_4 and T_5) insure reliable decoding at the SCBS (resp. MCBS). ■

VI. NUMERICAL RESULTS

We now provide numerical results for the rate region and the optimal quantization of the QF-JD and QF-WZTD schemes, which are identical by Theorem 4. We set same power for both UEs $P_1 = P_2$, while $P_r = 5P_1$ and the SCBS (resp. MCBS) has 50 (resp. 500) antennas. The path loss exponent $\alpha = 2.7$ and the inter-node distances in meters are: $d_{d1} = 105, d_{d2} = 110$, and $d_{dr} = 100$, while d_{r1} and d_{r2} are given in each figure. We define the received SNR at the MCBS from UE₁ as follows: $\text{SNR} = 10 \log_{10}(P_1(M-N)/d_{d1}^\alpha)$.

Fig. 3 compares the rate regions of massive MIMO HetNet under the proposed QF schemes, DF relaying, LTE-A (dual-hop DF scheme), direct transmission (without the SCBS) and

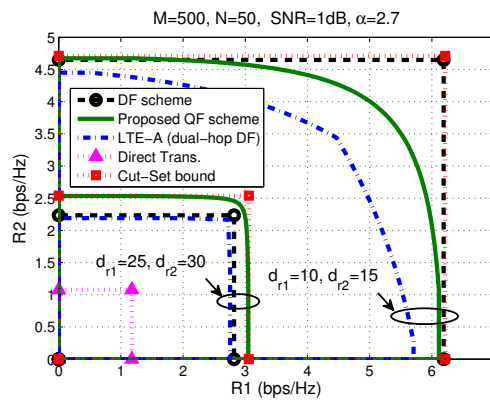


Fig. 3. Rate regions of different transmission schemes.

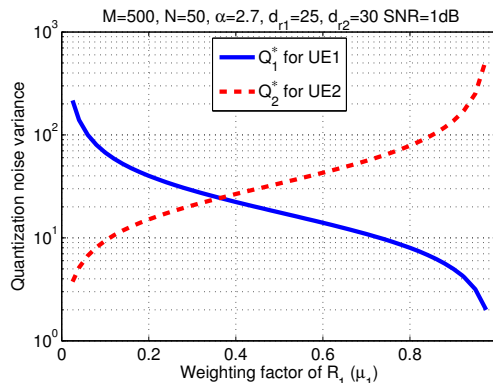


Fig. 4. Optimal quantization noise variances to maximize the weighted sum rate, for both QF-JD and QF-WZTD.

the cut-set outer bound [8]. Both the QF and DF schemes outperform the direct transmission and LTE-A schemes, due to deploying the SCBS in full-duplex mode and utilizing the direct links from UEs to the MCBS. However, neither DF nor QF is always preferred; QF relaying outperforms DF relaying when UEs move further from the SCBS, but underperforms DF relaying in the opposite case.

Fig. 4 shows the optimal Q_1^* and Q_2^* that maximize the weighted sum rate. As the weighting factor (μ_1, μ_2) of each UE rate increases, the SCBS performs finer quantization to send a clearer version of that UE's signal to the MCBS. Similar results hold for the optimal phase duration of QF-WZTD in Fig. 5. As μ_1 increases, the SCBS sends the quantization index of UE₁ over longer phase duration to increase its rate.

VII. CONCLUSION

We have investigated how massive MIMO impacts the up-link transmission design for a dense HetNet with ZF detection at the SCBS and MCBS and QF relaying at the SCBS. For rate maximization, we derived the optimal quantization parameters whose size was shown to be equal to the number of UEs instead of antennas as in regular MIMO systems, and we showed how their values depend on large-scale fading. Moreover, the MCBS can deploy simple separate and sequential decoding for each user's message while achieving the same rate region obtained with joint decoding. The simpler decoding technique is facilitated through Wyner-Ziv binning and multiple-timeslot transmission at the SCBS, which is conveniently optimized based on the quantization parameters.

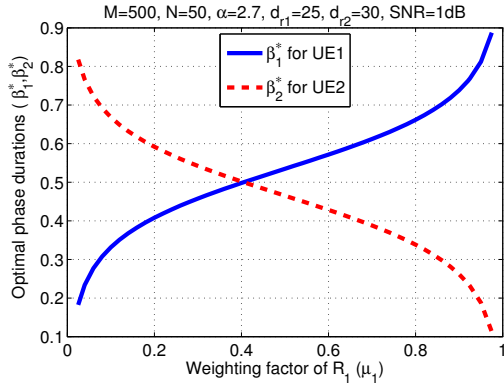


Fig. 5. Optimal phase durations to maximize the weighted sum rate of the QF-WZTD scheme.

APPENDIX A: PROOF OF THEOREM 1

The discrete memoryless MARC with orthogonal receivers (as in (3)) is specified by a collection of pmf $p(\tilde{\mathbf{y}}_{dr}|\mathbf{x}_r)$ $p(\tilde{y}_{d1}|x_1)p(\tilde{y}_{d2}|x_2)p(\tilde{y}_{r1}|x_1)p(\tilde{y}_{r2}|x_2)$. The $(2^{nR_1}, 2^{nR_2}, n, Pe)$ code follows standard definitions in [8]. We consider B independent transmission blocks each of length n . Two sequences of $B - 1$ messages $w_{1,j}$ and $w_{2,j}$ for $j \in [1 : B - 1]$ will be sent in nB transmissions. Hence, both UEs do not transmit in the last block (B) which reduces the rates by a factor of $1/B$ (negligible as $B \rightarrow \infty$) [8].

1) *Codebook generation*: The codebook generation can be explained as follows. First, fix the pmf $P^\dagger = p(x_1)p(x_2)p(\mathbf{x}_r)p(\hat{y}_{r1})p(\hat{y}_{r2})$ where $p(\mathbf{x}_r) = \prod_{i=1}^N p(x_{ri})$. Second, for each block $j \in \{1 : B\}$ and according to P^\dagger , randomly and independently generate 2^{nR_μ} codewords $x_\mu^n(w_{\mu,j})$ that encode $w_{\mu,j}$ where $\mu \in \{1, 2\}$. Third, similarly generate $2^{nR_{r1}}$ ($2^{nR_{r1}}$) codewords $\hat{y}_{r1,j}^n(l_j)$ ($\hat{y}_{r2,j}^n(k_j)$) that encode l_j (k_j), where R_{r1} (R_{r2}) is the transmission rate of l_j (k_j) by \mathcal{R} . Last, for each pair (l_{j-1}, k_{j-1}) , generate $2^{n(R_{r1}+R_{r2})}$ codewords $\mathbf{x}_r^n(l_{j-1}, k_{j-1})$ according to P^\dagger .

2) *Encoding*: Let $(w_{1,j}, w_{2,j})$ be the messages to be sent in block j . Then, UE₁ (UE₂) transmits $x_1^n(w_{1,j})$ ($x_2^n(w_{2,j})$). Moreover, since \mathcal{R} has already estimated $(\hat{l}_{j-1}, \hat{k}_{j-1})$ in block $j-1$, it transmits $\mathbf{x}_r^n(\hat{l}_{j-1}, \hat{k}_{j-1})$ in block j . In the same block, \mathcal{R} also utilizes $\tilde{y}_{r1}^n(j)$ and $\tilde{y}_{r2}^n(j)$ to find l_j and k_j such that

$$(\hat{y}_{r1}^n(l_j), \tilde{y}_{r1}^n(j)) \in A_\epsilon^n, \text{ and } (\hat{y}_{r2}^n(k_j), \tilde{y}_{r2}^n(j)) \in A_\epsilon^n, \quad (21)$$

respectively. By covering lemma [8], such l_j and k_j exist if

$$R_{r1} > I(\hat{Y}_{r1}; \tilde{Y}_{r1}) \triangleq \zeta_1 \text{ and } R_{r2} > I(\hat{Y}_{r2}; \tilde{Y}_{r2}) \triangleq \zeta_2. \quad (22)$$

3) *Decoding*: Without loss of generality, assume that all transmitted messages and quantization indices are equal to 1. Then, at the end of block $j + 1$, \mathcal{D} utilizes \tilde{y}_{d1}^n and \tilde{y}_{d2}^n in block j and $\tilde{\mathbf{y}}_{dr}$ in block $j + 1$ to find a unique message pair $(\tilde{w}_{1,j}, \tilde{w}_{2,j})$ for some quantization index pair $(\tilde{l}_j, \tilde{k}_j)$ such that $(x_1^n(\tilde{w}_{1,j}), \hat{y}_{r1}^n(\tilde{l}_j), \tilde{y}_{d1}^n(j)) \in A_\epsilon^n$, $(\mathbf{x}_r^n(\tilde{l}_j, \tilde{k}_j), \tilde{\mathbf{y}}_{dr}^n(j + 1)) \in A_\epsilon^n$, and $(x_2^n(\tilde{w}_{2,j}), \hat{y}_{r2}^n(\tilde{k}_j), \tilde{y}_{d2}^n(j)) \in A_\epsilon^n$. (23)

Let J_1, J_2 and J_3 be as follows:

$$J_i \triangleq I(\hat{Y}_{ri}; X_i, \tilde{Y}_{di}) + I(\mathbf{X}_r; \tilde{\mathbf{Y}}_{dr}), \quad i \in \{1, 2\} \quad (24)$$

$$J_3 \triangleq I(\hat{Y}_{r1}; X_1, \tilde{Y}_{d1}) + I(\hat{Y}_{r2}; X_2, \tilde{Y}_{d2}) + I(\mathbf{X}_r; \tilde{\mathbf{Y}}_{dr}).$$

Then, applying JT analysis [8] to (23) leads to some rate constraints, that are combined with (22) to obtain the constraints:

$$R_i \leq I(X_i; \tilde{Y}_{ri}, \tilde{Y}_{di}) \triangleq J_4, \quad i \in \{1, 2\} \quad (25)$$

$$R_i \leq I(X_i; \tilde{Y}_{di}) + J_i - \zeta_i \triangleq J_5,$$

$$R_i \leq I(X_i; \tilde{Y}_{di}) + J_3 - \zeta_1 - \zeta_2 \triangleq J_6, \text{ and}$$

$$R_1 + R_2 \leq I(X_1; \tilde{Y}_{d1}) + I(X_2; \tilde{Y}_{d2}) + J_3 - \zeta_1 - \zeta_2 \triangleq J_7.$$

In (25), J_5 is redundant since $J_6 < J_5$. We obtain I_1, \dots, I_5 in (6) by applying (25) to the channel in (3) with 1) the signaling in (4), 2) the approximations in [14] where

$$\|\mathbf{a}_{ri}\|^2 \rightarrow d_{ri}^{-\alpha}(N - 2) \approx d_{ri}^{-\alpha}N, \quad i \in \{1, 2\}, \quad (26)$$

$$\|\mathbf{a}_{dv}\|^2 \rightarrow d_{dv}^{-\alpha}(M - N - 2) \approx d_{dv}^{-\alpha}(M - N) \quad v \in \{1, 2, r\},$$

and 3) the equivalency of the rate $(I(\mathbf{X}_r; \tilde{\mathbf{Y}}_{dr}))$ from \mathcal{R} to \mathcal{D} to that from N single-antenna UEs to \mathcal{D} since $M \gg N$ [14].

REFERENCES

- [1] M. Jaber *et al.*, "5G backhaul challenges and emerging research directions: A survey," *IEEE Access*, vol. 4, pp. 1743–1766, May 2016.
- [2] M. Kamel, W. Hamouda, and A. Youssef, "Ultra-dense networks: A survey," *IEEE Commun. Surveys Tuts.*, vol. 18, no. 4, 2016.
- [3] G. Kramer, M. Gastpar, and P. Gupta, "Cooperative strategies and capacity theorems for relay networks," *IEEE Trans. Inf. Theory*, vol. 51, no. 9, pp. 3037–3063, Sept. 2005.
- [4] A. Abu Al Haija and C. Tellambura, "Small-Macro Cell Cooperation for HetNet Uplink Transmission: Spectral Efficiency and Reliability Analyses," in *IEEE J. Sel. Areas Commun.*, vol. 35, no. 1, Jan. 2017.
- [5] G. Zeitler, R. Koetter, G. Bauch, and J. Widmer, "An adaptive compress-and-forward scheme for the orthogonal multiple-access relay channel," in *IEEE PIMRC*, Sept. 2009.
- [6] M. Lei and M. R. Soleymani, "Diversity multiplexing tradeoff of the half-duplex slow fading multiple-access relay channel based on generalized quantize-and-forward scheme," *IEEE Wireless Commun. Lett.*, vol. 4, no. 1, pp. 74–77, Feb. 2015.
- [7] A. Winkelbauer, N. Goertz, and G. Matz, "Compress-and-forward in the multiple-access relay channel: with or without network coding?" in *IEEE ISTC*, Aug. 2012.
- [8] R. El Gamal and Y.-H. Kim, *Network Information Theory*, 1st ed. Cambridge University Press, 2011.
- [9] S. Simoens, O. Muoz-Medina, J. Vidal, and A. del Coso, "Compress-and-forward cooperative MIMO relaying with full channel state information," *IEEE Trans. Signal Process.*, vol. 58, pp. 781–791, Feb. 2010.
- [10] X. Lin, M. Tao, and Y. Xu, "MIMO two-way compress-and-forward relaying with approximate joint eigen-decomposition," *IEEE Commun. Lett.*, vol. 17, no. 9, pp. 1750–1753, Sep. 2013.
- [11] Y. Zhou and W. Yu, "Fronthaul compression and transmit beamforming optimization for multi-antenna uplink C-RAN," *IEEE Trans. Signal Process.*, vol. 64, no. 16, pp. 4138–4151, Aug. 2016.
- [12] E. Bjrnson *et al.*, "Massive MIMO: ten myths and one critical question," *IEEE Commun. Mag.*, vol. 54, no. 2, pp. 114–123, Feb. 2016.
- [13] B. M. Hochwald, T. L. Marzetta, and V. Tarokh, "Multiple-antenna channel hardening and its implications for rate feedback and scheduling," *IEEE Trans. Inf. Theory*, vol. 50, no. 9, pp. 1893–1909, Sept. 2004.
- [14] H. Q. Ngo, E. G. Larsson, and T. L. Marzetta, "Energy and spectral efficiency of very large multiuser MIMO systems," *IEEE Trans. Commun.*, vol. 61, no. 4, pp. 1436–1449, Apr. 2013.
- [15] E. Bjrnson, L. Sanguinetti, and M. Kountouris, "Deploying dense networks for maximal energy efficiency: small cells meet massive MIMO," in *IEEE J. Sel. Areas Commun.*, vol. 34, no. 4, Apr. 2016, pp. 832–847.
- [16] R. Mudumbai, D. Brown, U. Madhoo, and H. Poor, "Distributed transmit beamforming: challenges and recent progress," *IEEE Commun. Mag.*, vol. 47, no. 2, pp. 102–110, Feb. 2009.
- [17] D. Bharadia, E. McMillin, and S. Katti, "Full duplex radios," *ACM, SIGCOMM*, vol. 43, no. 4, pp. 375–386, Aug. 2013.
- [18] R. G. Gallager, *Information Theory and Reliable Communication*. New York:Wiley, 1968.